Interaction of Fluorescently Labeled Myosin Subfragment 1 with Nucleotides and Actin†

Raul Aguirre,‡ Frances Gonsoulin, and Herbert C. Cheung*
Department of Biochemistry, University of Alabama at Birmingham, University Station, Birmingham, Alabama 35294
Received May 9, 1986; Revised Manuscript Received July 15, 1986

ABSTRACT: Isolated myosin heads (subfragment 1) were modified by covalent attachment of 5-(iodoacetamido)fluorescein or 5-(iodoacetamido)salicylic acid to the essential sulfhydryl group SH_1. The extrinsic fluorescence of the modified proteins was sensitive to binding of nucleotides and F-actin. With the fluorescein derivative [subfragment 1 (S1) modified with 5-(iodoacetamido)fluorescein (IAF) at SH_1 (S1-AF)], association with MgADP decreased the probe fluorescence by 30%, whereas binding to actin increased the emission by a factor of 2. In the ternary complex acto–S1-AF·MgADP, the effect of nucleotide on the intensity of the attached fluorescein canceled the effect of actin. The fluorescence state of this ternary complex was similar to that of S1-AF·MgADP. The emission of S1-AF was resolved into two components with lifetimes of 4.3 and 0.6 ns and relative contributions of 33% and 67%, respectively. Interaction of S1-AF with nucleotides and actin did not alter the lifetimes but significantly shifted their fractional contributions. Quenching studies showed that the short lifetime likely arose from the fluorescein moiety statically quenched by internal groups. Binding of MgADP to the salicylate derivative [S1 modified with 5-(iodoacetamido)salicylic acid at SH_1 (S1-SAL)] induced a 25% enhancement of the probe fluorescence, whereas formation of acto–S1-SAL decreased the emission by 10% regardless of whether MgADP was bound to the protein. Both labeled S1 species bound MgADP with a similar affinity, comparable to that of unmodified S1 previously reported by other investigators. In the ternary complex acto–S1-SAL·MgADP, the probe sensed predominantly the effect of actin while in acto–S1-AF·MgADP the probe was sensitive to the effect of nucleotide. The results suggest that in the formation of actosubfragment 1 there is a loosening of the S1 heavy-chain structure in the region of SH_1. Nucleotide binding to actosubfragment 1 results in a reversal of the structural change, as reported by the fluorescein probe but not by the salicylate. These results are interpreted in terms of two states of the ternary complex actin·S1·ADP. The extrinsic probes of both labeled proteins also were used to demonstrate a slow transition of the ternary complex formed between labeled S1, MgADP, and vanadate. The rate constant for this transition was (5–7) × 10^{-3} s^{-1}.

Most of the current proposed mechanisms on the cyclic interactions of myosin with nucleotides and actin imply that in the myosin head the binding site of actin and that of nucleotide(s) are interconnected. Elucidation of the structural relationship between these two sites has been initiated by establishing a matrix of well-defined points within the myosin head and determining the changes in their relative positions induced by the binding of nucleotides and actin (Morales et al., 1982). These points include several specific amino acid residues and proteolytic cleavage points. Among these marker residues, one of the best characterized is a cysteine of the heavy chain of subfragment 1 whose sulfhydryl group is commonly called SH_1. Because of its high reactivity, SH_1 has been selectively modified by a variety of reagents, including fluorescent markers and spin-labels (Reisler, 1982). The relationship of SH_1 with the nucleotide binding site has been recognized since early studies showed that modification of this thiol with *N*-ethylmaleimide resulted in an increase of the Ca^{2+}-ATPase activity (Sekine & Kielley, 1964). There is nonetheless good evidence that SH_1 may not participate directly in ATPase catalysis (Wiedner et al., 1978) and that the activating effect of its modification on activity may be due to a structural distortion transmitted to the active site. This notion is strengthened by the observation that the degree of activation depends, to a certain extent, on the size of the group attached to SH_1 (Botts et al., 1979). Modification of SH_1 also reduces the activation of Mg^{2+}-dependent myosin ATPase by actin. These results show the close relationship between SH_1 and the actin and nucleotide binding sites and suggest that this thiol may occupy a key position in the path of intersite signal transmission. Some evidence is available indicating that SH_1 and the actin and nucleotide binding sites are reciprocally affected; that is, modification of SH_1 affects some properties of the two binding sites in chymotryptic myosin subfragment 1 (S1),[1] and actin and nucleotides can induce changes in the environment of SH_1. The evidence so far has been mainly provided by the observations that in the presence of ATP, the reactivity of SH_1 decreases and that actin binding also depresses the reactivity of SH_1 (Duke et al., 1976).

In this study, we used two different fluorescent probes covalently attached to SH_1 to detect perturbations in its environment induced by binding of nucleotides and of F-actin. Our results reveal that nucleotides and F-actin produced opposing effects upon the environment of SH_1. Since these two probes are sensitive to different environmental factors, they provide complementary information useful for investigating the nature

† This work was supported in part by a grant from the National Institutes of Health (AM31239).
* Correspondence should be addressed to this author.
‡ Present address: Department of Biochemistry, University of Chile, Santiago, Chile.

[1] Abbreviations: IAF, 5-(iodoacetamido)fluorescein; ISAL, 5-(iodoacetamido)salicylic acid; S1, chymotryptic myosin subfragment 1; TES, 2-[[tris(hydroxymethyl)methyl]amino]ethanesulfonic acid; S1-SAL, subfragment 1 modified with ISAL at SH_1; S1-AF, subfragment 1 modified with IAF at SH_1; SAL, acetamidosalicylate moiety; AF, acetamidofluorescein moiety; SDS, sodium dodecyl sulfate; 1,5-IAEDANS, *N*-(iodoacetyl)-*N'*-(5-sulfo-1-naphthyl)ethylenediamine; AMP-PNP, 5'-adenylyl imidodiphosphate.

0006-2960/86/0425-6827$01.50/0

and extent of microenvironmental changes in the region of SH_1, induced by actin and/or nucleotides.

Materials and Methods

Myosin was prepared from rabbit skeletal muscle by a procedure similar to that previously described by Flamig and Cusanovich (1981). This method involved a 1-h extraction in a phosphate buffer, pH 7.5, and 0.3 M KCl followed by successful fractionations in 0.5 M KCl, pH 7.0. Subfragment 1 was obtained by digestion of myosin with chymotrypsin, followed by purification on a DEAE-cellulose (DE-52) column (Weeds & Taylor, 1975). The two isozymes S1(A1) and S1(A2) were pooled for subsequent labeling with fluorescent probes. Actin was prepared from acetone powder of rabbit skeletal muscle according to Spudich and Watts (1971) and polymerized as described previously (Cheung et al., 1983). Polymerized actin was extensively dialyzed in 60 mM KCl and 30 mM TES at pH 7.5 (buffer A) for 24 h and used immediately in actosubfragment 1 studies.

The concentration of S1 was estimated from an absorbance of 0.75 g^{-1} cm^{-1} at 280 nm (Wagner & Weeds, 1977) and a molecular weight of 115000. An absorbance of 0.63 g^{-1} cm^{-1} at 290 nm (Houk & Ue, 1974) and a monomeric molecular weight of 42000 were used to determine the concentration of F-actin.

S1 was labeled at SH_1 with IAF or ISAL in buffer A by using a 1.2 molar excess of the reagents. Prior to labeling, the protein solution (7 mg/mL) was first dialyzed in buffer A. Appropriate volumes of 3 mM ISAL (dissolved in buffer A) or 1 mM IAF (dissolved in 1:1 methanol–buffer A) were then added to S1 followed by incubation at 4 °C for 18 h in the dark. Unreacted probe was subsequently removed by exhaustive dialysis in buffer A. The degree of labeling with IAF was determined according to Marsh and Lowey (1980), and quantitation of bound ISAL was made by measuring the absorbance at 323 nm of the labeled protein and subtracting the absorbance of an equivalent concentration of unmodified S1 at this wavelength. For this purpose, concentrations of labeled and unlabeled S1 were measured by the method of Lowry et al. (1951). A molar extinction coefficient (323 nm) of 3070 M^{-1} cm^{-1} was used to estimate the amount of bound ISAL. The kinetics and extent of labeling were also followed by measurements of Ca^{2+}-activated ATPase activities (Cheung et al., 1983), and the homogeneity of the labeled protein was assessed by SDS–polyacrylamide gel electrophoresis of intact and partially trypsin-digested S1 (Cheung et al., 1983).

Steady-state fluorescence measurements were performed on either a Perkin-Elmer 650-40 ratio spectrofluorometer thermostated at 20 ± 0.1 °C and equipped with a magnetic stirrer or a Perkin-Elmer MPF-66 spectrofluorometer. Fluorescence lifetimes were determined in a PRA pulse nanosecond fluorescence spectrometer. The decay curves were deconvoluted by a nonlinear least-squares program which included correction for nonrandom error introduced by sample scattering. Measurement details, data collection procedures, and fitting algorithm and statistics have been described elsewhere (Cheung et al., 1983). The Durbin–Watson number (Durbin & Watson, 1951) was also used in the present study to provide an additional evaluation of the goodness of exponential fits. For ISAL-labeled proteins, a Ditric three-cavity 340-nm interference filter (half-maximum bandwidth 13.5 nm) was used for excitation, and a three-cavity 430-nm interference filter (half-maximum bandwidth 7.3 nm) was used to isolate the emission. Three-cavity interference filters were also used for IAF-labeled proteins: 490 nm (bandwidth 7.3 nm) for excitation and 520 nm (bandwidth 8.2 nm) for emission.

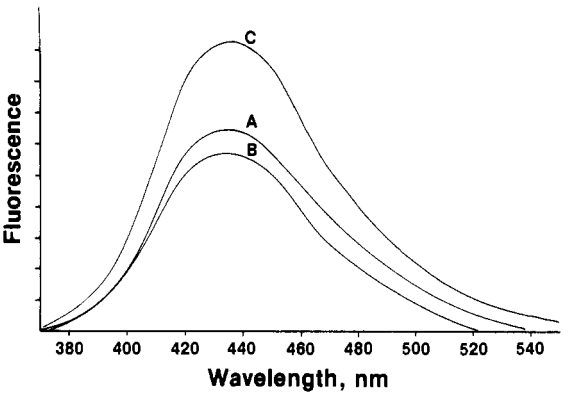

FIGURE 1: Corrected emission spectra of S1-SAL, acto–S1-SAL, and S1-SAL·ADP. The excitation wavelength was 340 nm. The spectra were recorded at 20 °C with the proteins in buffer A and 2 mM $MgCl_2$. (A) S1-SAL (4.5 μM); (B) acto–S1-SAL (4.5 μM F-actin plus 4.5 μM S1-SAL); (C) S1-SAL·ADP (15 μM ADP plus 4.5 μM S1-SAL).

IAF and ISAL were purchased from Molecular Probes (Junction City, OR). Trypsin, soybean trypsin inhibitor, ADP, and ATP were obtained from Sigma Chemical Co. (St. Louis, MO). A stock solution (100 mM) of sodium vanadate was prepared from V_2O_5 (Aldrich Chemical Co., Milwaukee, WI) according to Goodno (1982).

Results

Labeling of S1 with ISAL and IAF. Under the labeling conditions established in the present study, 0.8–0.9 mol of ISAL or IAF was attached per mole of S1 as estimated by absorbance measurements. In agreement with the results obtained with several other reagents covalently attached to SH_1 (Reisler, 1982), S1 displayed an increased Ca^{2+}-ATPase activity after labeling with these fluorescent probes. Modification by IAF and ISAL produced a 3-fold and 5-fold activity increase, respectively. Specificity of the labeling was also verified by SDS electrophoresis of labeled S1 partially digested by trypsin. The gels showed a single fluorescent band in the 20K peptide in which SH_1 is located. We estimated that not less than 90% of the labels attached to the protein were bound to SH_1.

Fluorescence Properties of S1-SAL. The fluorescence intensity of S1-SAL increased by about 25% upon formation of binary complexes with ADP, ATP, or pyrophosphate with no noticeable shift of the emission maximum at 438 nm (Figure 1). Association of F-actin with S1-SAL, on the other hand, decreased the fluorescence intensity by about 10% and produced a slight blue shift of 2 nm in the emission maximum. The fluorescence increase resulting from nucleotide binding was abolished when actin was added to S1-SAL·ADP. The final fluorescence level was below that of S1-SAL, as depicted in Figure 2A. This level of fluorescence was similar to that observed with acto–S1-SAL. Addition of ADP to acto–S1-SAL did not produce any change in the SAL intensity. The SAL label in S1-SAL spectrally sensed two S1 conformations: one induced by nucleotide and the other in rigor acto–S1 in the absence of bound MgADP. However, it did not discriminate between acto–S1 that contained MgADP and that which did not. When a large excess of ATP was added to acto–S1-SAL, a rapid increase in fluorescence was observed. This intensity was reasonably stable for about 2 min and then began to decay rapidly over about 30 s (Figure 2A). The final level of the SAL fluorescence was slightly higher than that observed with acto–S1-SAL prior to addition of ATP. The time interval over which the intensity remained high and stable could be

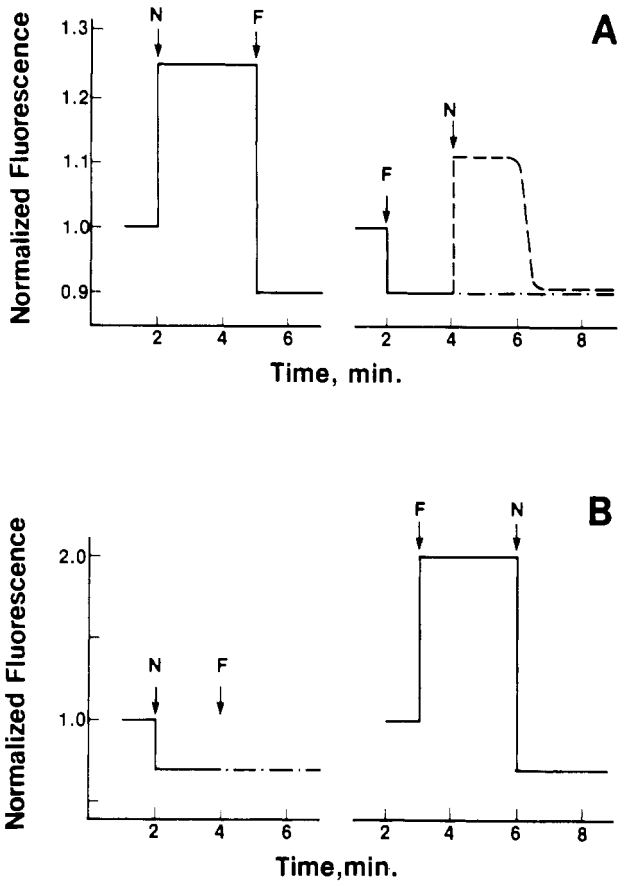

FIGURE 2: Effect of sequential additions of nucleotides and actin on the fluorescence of S1-SAL (A) and S1-AF (B). (A) 2.8 μM S1-SAL in buffer A + 2 mM $MgCl_2$, pH 7.5. Emission was monitored at 430 nm with excitation at 340 nm. N denotes the addition of nucleotides (10 μM ADP or 200 μM ATP), and F denotes the addition of F-actin (5.8 μM). Right panel: (--) fluorescence immediately following addition of ATP; (-·-) fluorescence following addition of ADP. (B) S1-AF fluorescence was monitored at 520 nm with excitation at 490 nm. All other conditions were identical with those given in (A).

lengthened or shortened by increasing or decreasing the ATP concentration. The observed rapid fluorescence increase induced by ATP was related to dissociation of the actosubfragment 1 complex since the fluorescence level of undissociated S1-SAL was not affected by nucleotide. The amplitude of this increase was only about 50% of that induced by addition of nucleotides (ADP or ATP) to S1-SAL. These results are compatible with the notion that during steady-state ATP hydrolysis by actomyosin a substantial fraction of myosin remains undissociated from actin. If the assumption is made that complete dissociation of S1-SAL by ATP from acto–S1-SAL should result in a fluorescence increase of 25%, the results would suggest that about 50% of the S1-SAL remained undissociated from actin during the steady state. The rapid fluorescence decrease which occurred after 2 min reflects reassociation of S1-SAL with actin as substrate was being depleted. The final fluorescence level reflects acto–S1-SAL in which the products of ATP hydrolysis, P_i and ADP, remained bound to the active site of the S1-SAL.

Fluorescence Properties of S1-AF. In contrast to the effect of nucleotides and pyrophosphate on the fluorescence intensity of S1-SAL, complex formation of these ligands with S1-AF induced a decrease in the fluorescence intensity of this probe by about 30%, which was accompanied by a small red shift (1.5 nm) of the emission maximum when excited at 490 nm. Addition of actin to this S1-AF·ADP had no effect on the AF fluorescence. On the other hand, addition of actin to S1-AF in the absence of nucleotide produced a 2-fold increase in fluorescence. This enhancement was abolished upon addition of ADP. The final fluorescence level in the system containing actin, S1-AF, and MgADP was identical with that observed with S1-AF·ADP. These results are summarized in Figure 2B. Like SAL, the probe fluorescein reported two S1 conformations: one induced by nucleotide and the other induced by rigor acto–S1 formation. The unattached S1-AF·ADP was in a low fluorescence state, while acto–S1-AF was in a high fluorescence state. The probe was sensitive to perturbation of S1 in the rigor complex by nucleotide binding to S1.

Table I: Effect of Polyvalent Anions on the Fluorescence of S1-AF and Acto–S1-AF[a]

anion	fluorescence	
	S1-AF	acto–S1-AF
none	100	200
sodium phosphate	77	152
sodium pyrophosphate	73	73
sodium sulfate	74	146
potassium oxalate	78	153

[a] The fluorescein fluorescence was measured with 2.5 μM S1-AF in buffer A plus 2 mM $MgCl_2$. Emission wavelength was 520 nm and excitation wavelength 490 nm. All anion concentrations were 2 mM. Acto–S1-AF was prepared by mixing 2.5 μM S1-AF with 5.0 μM F-actin.

Our results on S1-AF differed from those recently reported by Ando (1984) in two major aspects. He observed no spectral change in S1-AF upon addition of nucleotides, whereas we detected a 30% decrease in the fluorescein fluorescence. This apparent discrepancy is due to the presence of SO_4^{2-} in Ando's system. He reported a single lifetime around 4 ns for the labeled protein. Our decay data could not be fitted to a single-exponential function but were best fitted to a biexponential function as will be presented in a following section. We found that 2 mM SO_4^{2-} was sufficient to quench the fluorescence of S1-AF to about the same extent as ADP, ATP, or pyrophosphate did in the absence of SO_4^{2-}. Addition of the ligands to solutions of S1-AF containing SO_4^{2-} did not produce any change in the fluorescence as originally reported (Ando, 1984). Other polyvalent anions (Table I) also produced an effect similar to that of SO_4^{2-}. Although the maximum decrease of fluorescence attainable with nucleotides and the anions was very similar, this effect saturated at micromolar concentrations of nucleotides and pyrophosphate and at millimolar concentrations of the anions. In the ternary complex formed between S1-AF, ADP, and actin, the effect of nucleotide on the environment of the fluorophore was dominant over the effect of F-actin, in general agreement with Ando's results. Pyrophosphate acted similarly to ADP in abolishing the actin-induced fluorescence enhancement, but the other anions did not interfere with the effect of actin. Concerning the effect of sulfate and other anions, it should be mentioned that they induced a small increase (2–4%) in the SAL fluorescence in S1-SAL but this effect was not additive to the ADP effect already presented (i.e., the maximum ADP-induced enhancement of SAL fluorescence was still only about 25% when measured in the presence of sulfate or phosphate). Pyrophosphate, however, did induce an enhancement approaching that caused by ADP.

Interaction of ADP with S1-SAL, S1-AF, and Acto–S1-AF. The increase and the decrease in fluorescence induced by ADP in S1-SAL and S1-AF, respectively, enabled us to titrate both fluorescent S1 species with ADP (Figure 3). The shape of the titration curves was approximately hyperbolic, reaching saturation at a protein–ligand stoichiometry of approximately

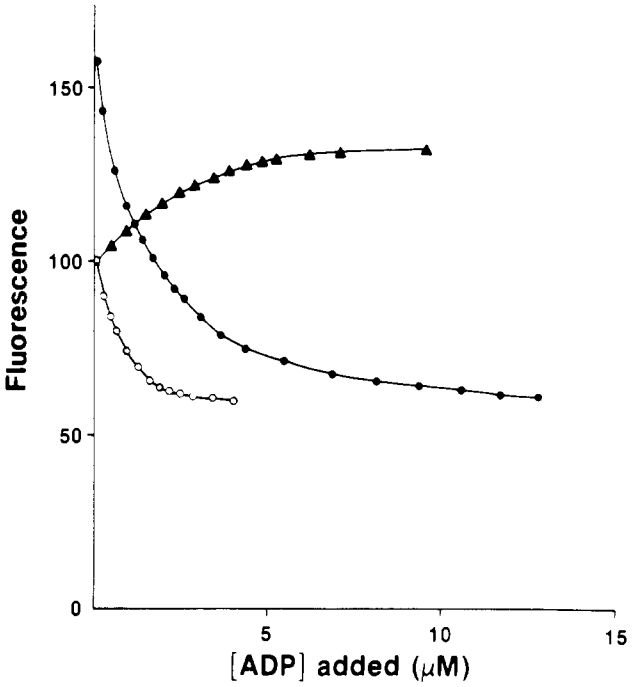

FIGURE 3: Titration of labeled S1 and acto-labeled S1 with ADP. Small volumes of 100 μM ADP were successively added to (○) S1-AF (2.5 μM), (●) acto–S1-AF (5 μM F-actin plus 2.5 μM S1-AF), and (▲) S1-SAL (4.6 μM). All measurements were carried out in buffer A plus 2 mM $MgCl_2$, pH 7.5 at 20 °C. Measured intensities were normalized with respect to the initial values of S1-SAL and S1-AF. The fluorescence was measured at 430 nm with excitation at 340 nm in (▲). In (○, ●), the fluorescence was measured at 520 nm with excitation at 490 nm.

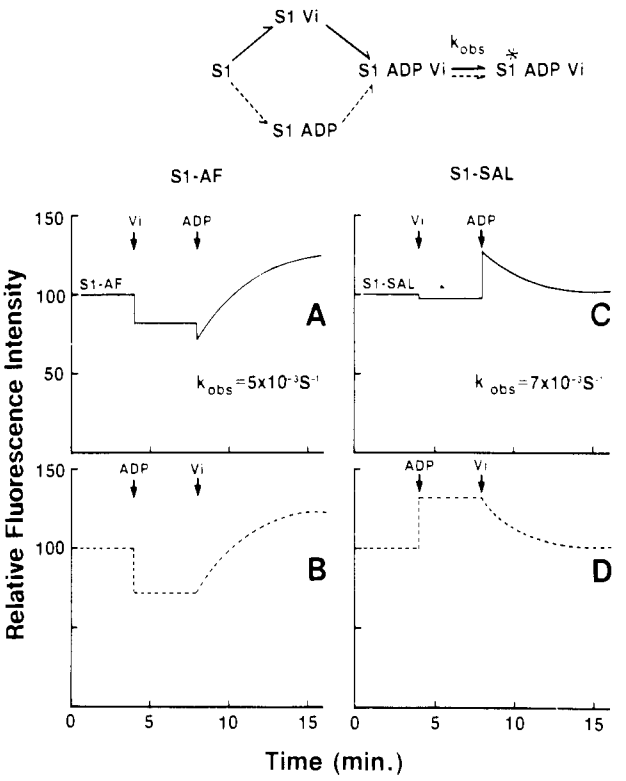

FIGURE 4: Fluorescence changes in labeled S1 induced by ADP and vanadate. 20 μM ADP and 100 μM vanadate were added in different sequences to 2 μM S1-AF (A and B) and to 4.4 μM S1-SAL (C and D). The readings were normalized to a value of 100 for the protein prior to the addition of ligands. In panels A and B, 490 and 520 nm were the excitation and emisson wavelengths, respectively. For panels C and D, the excitation was 340 nm, and the emission was measured at 430 nm. All the measurements were performed at 20 °C in buffer A plus 2 mM $MgCl_2$, pH 7.5.

1:1. The results are consistent with a single high-affinity binding site in the two labeled proteins for ADP. From the half-maximum change in fluorescence, an apparent dissociation constant for ADP was obtained: 1.01 μM for S1-SAL and 0.6 μM for S1-AF. These constants are in good agreement with previously published data obtained with unmodified S1 (Konrad & Goody, 1982) and suggest that modification of S1 by IAF or ISAL did not significantly affect the affinity of the protein for the nucleotide. A titration curve of acto–S1-AF is also presented in Figure 3. The dissociation constant of acto–S1-AF for ADP was estimated to be 1.6 μM, in reasonable agreement with previous data (0.5 μM) from acto–S1-AF (Ando, 1984). The small difference could arise from some contamination of F-actin with nucleotides. ADP titrations of acto–S1-SAL were not carried out since binding of ADP did not produce any change in the fluorescence of the rigor complex with this labeled protein.

Titration curves (not shown) of S1-AF with F-actin exhibited a slight sigmoidal shape which could be explained by a preferential binding of F-actin to some fraction of unlabeled S1. This could account for the initial lag in the titration. Consistent with this explanation, it was also observed that sigmoidicity was increased by increasing the fraction of unlabeled S1. As was previously observed (Ando, 1984), our results indicate that labeling of S1 with IAF decreased the affinity of F-actin for S1. This sigmoidal shape was also observed in the titration of S1-SAL and S1-SAL·ADP with F-actin as monitored by fluorescence decrease (results not shown). These results suggest that modification of SH_1 with ISAL also perturbed the interaction of S1 with actin to some extent.

Interaction of Vanadate with Labeled S1·ADP Complexes. It has been proposed that addition of vanadate (Vi) to a myosin–ADP complex produces a stable ternary state which mimics the transient myosin–products intermediate of the ATP hydrolysis (Goodno, 1982). It was of interest to determine whether S1·ADP could be distinguished from the ternary complex S1·ADP·Vi by using the fluorescent species S1-SAL and S1-AF. Figure 4 shows the changes in fluorescence intensity as a function of time upon sequential addition of Vi and ADP. With S1-AF, addition of Vi to the labeled S1 induced a 20% rapid reduction in fluorescence. Subsequent addition of ADP produced an additional rapid decrease to a final amount of about 30%, followed by a slow reversal of the intensity to a level about 30% higher than that of S1-AF (Figure 4A). If ADP was added first, subsequent addition of Vi did not produce any further change; instead, it induced a slow reversal of the intensity (Figure 4B). The rate constant for the slow fluorescence increase and the amplitude of this increase were independent of the order of addition of Vi and ADP. These results suggest that the ternary complex S1-AF·ADP·Vi was rapidly formed, followed by a slow transition to a state in which the AF moiety had a larger fluorescence than any of the four species S1-AF, S1-AF·Vi, S1-AF·ADP, or S1-AF·ADP·Vi. S1 in this final state of the ternary complex was different from S1 or S1·ADP. The fluorescein label sensed the formation of the binary complex S1-AF·Vi, but in the initial ternary complex, the probe reported predominantly bound ADP since the decreased fluorescence induced by ADP in S1-AF·ADP did not decrease further upon addition of Vi. The sensitivity of fluorescein to the S1 conformation induced by ADP in S1-AF·ADP·Vi parallels its similar sensitivity in acto–S1-AF·ADP. While the fluorescence change was in the opposite direction, a similar kinetic pattern was observed following formation of the ternary complex S1-SAL·ADP·Vi

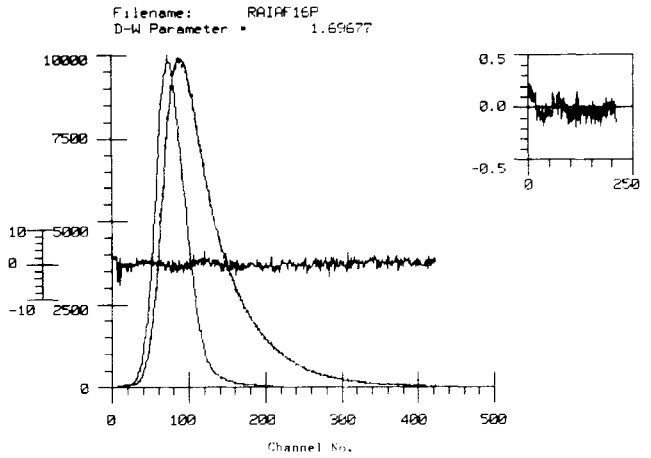

FIGURE 5: Fluorescence decay of S1-AF. The decay data were fitted to a biexponential function. The sharp peak on the left is the lamp profile. The solid curve is the best fit of the data with lifetimes of 4.17 and 0.48 ns and corresponding fractional amplitudes of 0.3 and 0.7, respectively. Each channel corresponds to 0.079 ns. The inset shows the autocorrelation function of the weighted residuals. The middle tracing across the plot shows the deviation between the calculated values and observed data. Also shown in the plot is the Durbin–Watson (D–W) parameter for the fit. A value of 1.75 indicates perfect fitting of the data to a biexponential function. The horizontal channel scale was shifted so that the zero channel shown in the figure actually corresponded to the channel at which data fitting began.

Table II: Effect of F-Actin and ADP on the Lifetimes of S1-AF[a]

species	τ_1 (ns)	α_1	τ_2 (ns)	α_2	χ_R^2
S1-AF	4.25 ± 0.06	0.33	0.57 ± 0.08	0.67	1.75
acto–S1-AF	4.42 ± 0.04	0.70	0.67 ± 0.10	0.30	1.00
S1-AF·ADP	4.24 ± 0.05	0.24	0.54 ± 0.04	0.76	1.51
acto–S1-AF·ADP	4.18 ± 0.05	0.30	0.74 ± 0.05	0.70	1.00

[a] The lifetimes were measured at 14 °C in buffer A plus 2 mM $MgCl_2$. S1-AF concentration was 5 μM, F-actin concentration was 10 μM, and ADP concentration was 50 μM.

(Figure 4C,D). The rate constant for the slow transition was 5×10^{-3} s^{-1} with S1-AF and 7×10^{-3} s^{-1} with S1-SAL. The similarity of the rate constants suggest that both probes sensed the same transition to a common species. A slow transition of the ternary complex formed from myosin, ADP, and Vi was previously suggested (Goodno, 1979) on the basis of the inhibition of myosin ATPase by Vi. From the rate of inhibition, these workers deduced a rate constant for M·ADP·Vi → M*·ADP·Vi. Their result was in good agreement with our rate constants measured directly with fluorescently labeled subfragment 1.

Accessibility of S1-SAL, S1-AF, and Acto–S1-AF. In order to better characterize the changes in the microenvironment of the fluorophores attached to SH_1 induced by F-actin and ADP, we performed time-resolved fluorescence decay measurements on S1-AF and S1-SAL. Shown in Figure 5 is the biexponential emission decay of S1-AF. The effect of ADP and F-actin on the decay pattern is summarized in Table II. Two lifetimes of about 4.2 and 0.6 ns were observed in all four species. In S1-AF alone, the major fractional contribution (α) was that of the short-lifetime component, whereas rigor formation of S1-AF with actin significantly shifted the contributions in favor of the long lifetime. On the other hand, ADP induced a slight shift of the amplitudes toward the short component. When ADP was added to acto–S1-AF, the fractional contributions were shifted to values approaching those of S1-AF·ADP alone. In spite of the shifts of the fractional contributions of the two components, the two lifetimes remained essentially unchanged. The pattern of the shifts of amplitude induced by ADP and actin followed the same pattern of changes of steady-state intensity induced by the same ligands. The existence of two lifetimes is not an intrinsic property of the fluorophore but a consequence of the microenvironment of the fluorophore in the protein. Extensive digestion of S1-AF with trypsin resulted in an increase of α to 0.9 in favor of the 4.2-ns component. In the adduct β-mercaptoethanol–AF, the probe decayed monoexponentially with the single lifetime equal to 4.2 ns. Thus, the short component observed with S1-AF and its complexes did not arise from an instrumental problem or analysis error. The emission decay of S1-SAL was also biexponential (Table III), with a major component of about 9.6 ns and a minor component of about 3 ns. ADP seemed to increase both SAL lifetimes slightly with a small shift of the amplitude toward the long component. These changes are in contrast with the lack of any apparent effect of actin on the decay parameters of S1-SAL (data not shown).

Table III: Fluorescence Lifetimes of S1-SAL[a]

species	τ_1 (ns)	α_1	τ_2 (ns)	α_2	χ_R^2
S1-SAL	9.60 ± 0.13	0.80	2.82 ± 0.63	0.20	1.00
S1-SAL·ADP	10.1 ± 0.24	0.87	3.90 ± 1.7	0.13	1.23

[a] The measurements were done at 14 °C in buffer A plus 2 mM $MgCl_2$. S1-SAL concentration was 4.4 μM, and ADP concentration was 15 μM.

Conformational changes induced by ADP and F-actin in S1 were also studied in terms of the accessibility of the fluorophores attached to SH_1 to external quenchers. Since the neutral quencher acrylamide is not effective in quenching IAF itself, quenching studies with S1-AF were carried out using KI. The quenching by I^- of the steady-state fluorescence of S1-AF, acto–S1-AF, and S1-AF·ADP is presented in Figure 6A in the form of Stern–Volmer plots. The effect of iodide on S1-AF·ADP is essentially indistinguishable from that on S1-AF. The nonlinear quenching pattern indicates fluorescence heterogeneity and negative deviation often found in systems with more than one lifetime. This heterogeneity was confirmed by the two lifetimes reported in Table II. The quenching of acto–S1-AF was considerably higher than for the other two species, and its Stern–Volmer plot displays a rather constant slope. The larger quenching suggests that the attached probe was more accessible to solvent collision in acto–S1-AF than in unattached S1. Since two lifetimes were also observed with acto–S1-AF, the apparent linearity is likely due to the fact that the short component represented less than 10% of the total emission. This small contribution of one component could give rise to the observed constant slope. The apparent Stern–Volmer constant (K_{sv}) for acto–S1-AF is 4.1 M^{-1}.

To gain insight into the origin of the observed quenching pattern, we also measured the lifetimes of S1-AF and acto–S1-AF as a function of iodide concentration. The reciprocals of the short lifetimes are plotted against $[I^-]$ in Figure 6B and the reciprocals of the long lifetimes in Figure 6C. For collisional quenching, the relationship of the plots shown in these figures is given by

$$1/\tau = 1/\tau_0 + k_q[Q]$$

where τ is the fluorophore lifetime observed at a given quencher concentration [Q], τ_0 is the lifetime in the absence of quencher, and k_q is the bimolecular Stern–Volmer rate constant for collisional quenching (Stern & Volmer, 1919). Since $K_{sv} = k_q\tau_0$, a value of the Stern–Volmer constant can be derived from lifetime measurements. The apparent negative slope displayed in Figure 6B for the short lifetimes probably

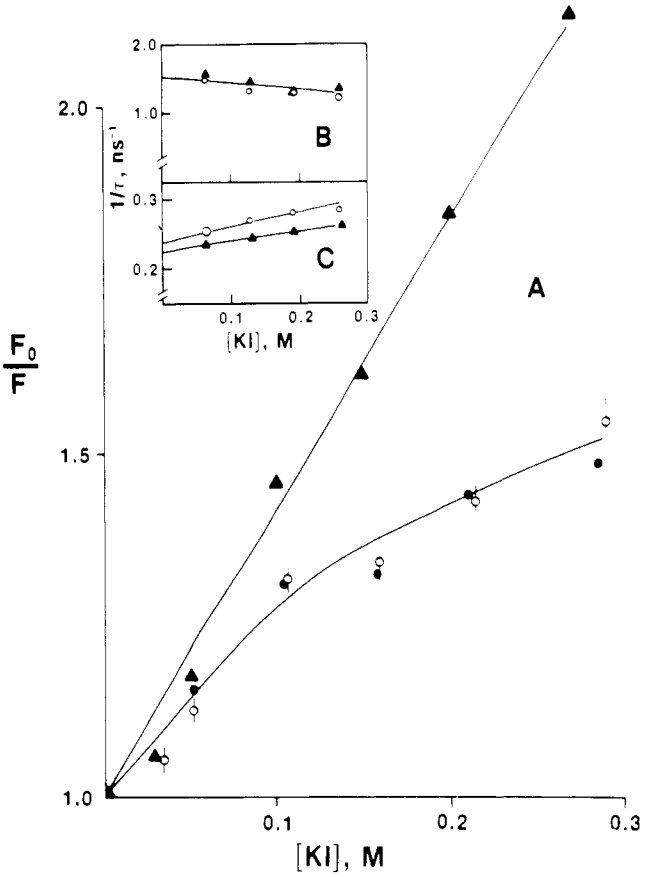

FIGURE 6: Stern–Volmer plots for the quenching by KI of the emission of S1-AF, acto–S1-AF, and S1-AF·ADP. In (A), F_0 was the fluorescence intensity measured at 520 nm with 490-nm excitation measured in the absence of the quencher, and F was the fluorescence intensity measured in the presence of quencher. (○) S1-AF (1.5 μM) alone; (●) S1-AF·ADP (1.5 μM S1-AF plus 1.5 mM ADP); (▲) acto–S1-AF (1.5 μM S1-AF plus 5 μM F-actin). The error bars given for S1-AF were obtained from duplicates. The insets show the effect of I^- on the short (B) and long (C) lifetimes of 5 μM S1-AF (○) and acto–S1-AF (▲) (2.5 μM S1-AF, 5 μM F-actin). The quenching experiments were performed at 14 °C in 30 mM TES and 2 mM $MgCl_2$, pH 7.5, and a constant ionic strength of 0.4.

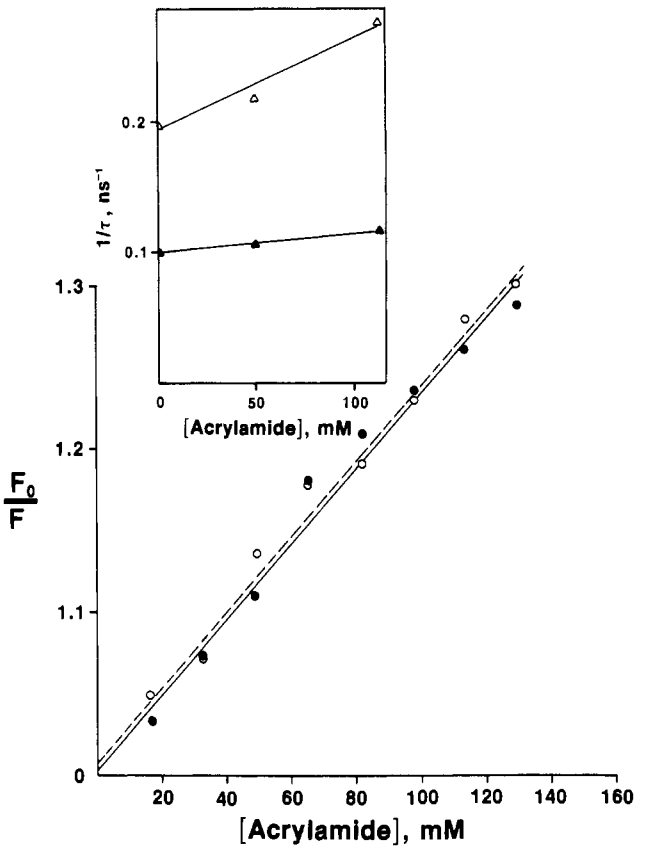

FIGURE 7: Stern–Volmer plots for the quenching of the fluorescence of S1-SAL and S1-SAL·ADP by acrylamide. The fluorescence intensity was measured at 430 nm with excitation at 340 nm. (○) S1-SAL (4.4 μM); (●) S1-SAL·ADP (4.4 μM S1-SAL plus 15 μM ADP). The inset shows the effect of acrylamide on the long (▲) and the short (△) lifetime of S1-SAL. Measurements were performed at 14 °C in buffer A, pH 7.5, with 2 mM $MgCl_2$.

reflects the relatively large error in the small lifetime values. As a first approximation, k_q for this component could be taken as zero. This approximation would require the quenching of the component to be largely static. The value of k_q for the long-lifetime component of acto–S1-AF is 1.4×10^8 M^{-1} s^{-1}, and the corresponding $K_{sv} = 0.58$ M^{-1}. This value is only a small fraction of the value obtained from steady-state intensity measurements. Thus, static quenching contributed substantially to the observed quenching pattern.

Stern–Volmer plots for the quenching of S1-SAL and S1-SAL·ADP by acrylamide are shown in Figure 7. The pattern of quenching revealed by steady-state intensity was very similar for both species. A single value of 2.3 M^{-1} was obtained for K_{sv}. From the $1/\tau$ vs. [acrylamide] plot of S1-SAL, a value of $K_{sv} = k_q\tau_0 = 1.1$ M^{-1} was obtained from the long-lifetime component and a value of $k_q\tau_0 = 3.5$ M^{-1} for the short-lifetime component. Since the fractional amplitudes of the long and short lifetimes were 0.8 and 0.2, respectively, a simple weighted average of the two values of K_{sv} derived from lifetimes is 1.6 M^{-1}, in reasonable agreement with steady-state results. The quenching of the SAL fluorescence is essentially dynamic in nature.

DISCUSSION

When IAF becomes attached to the SH_1 of S1, its quantum yield decreases by about 4-fold when compared with β-mercaptoethanol–AF. This high degree of quenching, which has been previously reported, can be reversed after extensive fragmentation of the protein by tryptic digestion (Ando, 1984). This finding is in accord with our observation that limited tryptic digestion of S1-AF to produce S1 heavy chain fragmented at two sites (Mornet et al., 1979) did not significantly change the fluorescence intensity but more extensive digestion resulted in a shift of the short-lifetime component toward the long-lifetime component. Since the present quenching studies suggest that the short-lifetime component in native S1-AF is likely quenched by a static mechanism, this static quenching is released by the disruption of the S1 structure. Thus, the fluorescein moiety must be extensively and statically quenched by neighboring groups surrounding the SH_1. While such a static quenching was previously suggested (Ando, 1984) on the basis of intensity changes, the present results provide evidence more directly indicating static quenching of AF in S1 through resolution of its emission decay into two components. When ADP binds to S1-AF, the static quenching becomes slightly enhanced, presumably through enhanced ground-state interaction between the probe and internal quenching groups, thus resulting in a decrease in the steady-state intensity and an increase in the fractional contribution of the short-lifetime component to the total emission.

In contrast to S1-AF, disruption of the S1 structure in S1-SAL by extensive tryptic digestion exposes the salicylate moiety, leading to enhanced collisional quenching with solvent. Nucleotide binding to native S1-SAL provides some protection of the probe and decreases its accessibility, resulting in higher

emission. The opposing effect of nucleotides on the emission of the two probes attached to S1 is a consequence of the intrinsic properties of the fluorophores and also dependent upon their average orientation with respect to neighboring groups. Their responses to nucleotide binding likely reflect localized conformational changes rather than global changes. This localized change appears to have a minimal effect on the ability of the labeled S1 to bind ADP. The fact that the covalent labels do induce a large enhancement in the Ca-ATPase activity would suggest the role of SH_1 to be on kinetic steps other than substrate binding.

Although both ISAL and IAF were attached to SH_1 of S1, they respond spectrally to binding of ADP and actin in different ways. S1-SAL senses only a single fluorescence state of the region of SH_1 in the acto–subfragment 1 rigor complex. This state is independent of ADP binding. The signal in acto–S1-SAL·ADP appears to be determined primarily by the linkage between subfragment 1 and actin. Any modification of this linkage by nucleotide binding to S1 does not seem sufficient to alter the environment surrounding the covalent label. Alternatively, the result could be explained by the existence of only one localized S1 conformation in acto–subfragment 1 irregardless of the presence of bound nucleotide. This interpretation would suggest the lack of a reciprocal influence between the nucleotide and actin binding sites in S1. However, the results from S1-AF show the existence of two fluorescence states of S1 in acto–S1-AF: a high fluorescence state associated with rigor complex without bound nucleotide and a low fluorescence state associated with rigor complex containing bound nucleotide. The environment of AF at SH_1 in the ternary rigor complex acto–S1-AF·ADP is similar to that of unattached S1-AF·ADP. This observation of two conformational states of acto–S1-AF dependent upon the presence of bound ADP is in general agreement with Ando (1984). However, our results indicate that the state of S1-AF in acto–S1-AF·ADP is not similar to S1-AF as Ando has shown. This discrepancy is due to external quenching of the fluorescein fluorescence in S1-AF by sulfate ions in his system. Thus, in acto–S1-AF·ADP, the fluorescein fluorescence is largely determined by bound nucleotide and not by contacts between S1 and actin as in the case of acto–S1-SAL·MgADP. We cannot establish whether the sensitivity of the fluorescein moiety toward nucleotide binding is related to its bulky size as compared to salicylate or to possible interaction between the nucleotide site and the SH_1 region. The possibility of such an interaction remains an open question because we (Cheung et al., 1985) have recently shown that the separation between the two regions can be as small as 15 Å. As has been discussed (Ando, 1984), the results obtained from S1-AF support the notion of communication between the nucleotide and actin binding sites in myosin. This reciprocal effect is relayed through a region where the SH_1 is located. While SH_1 has been known as a convenient marker for sensing the interaction between actin and myosin, it is only within the past 2 years that unequivocal evidence (Muhlrad & Morales, 1984; Katoh et al., 1985) is available showing the thiol group to be located within a short segment of the S1 heavy chain which may in fact be the strong actin binding site. This close proximity makes SH_1 a strategic marker for sensing perturbation resulting from interaction with actin.

The general effect of actin on the fluorescence of S1-SAL and S1-AF is similar in one aspect. Upon tryptic digestion, the intensity of S1-AF increased (Ando, 1984), and the intensity of S1-SAL decreased (present work). These changes are in the same directions observed when the respective labeled S1 was complexed with actin. Formation of the actin–S1 linkage must result in a loosening of the S1 heavy-chain structure. This change leads to a more open structure in the region of SH_1 which is responsible for the different observed spectral responses of the two probes. Both probes sense the same kind of structural change of S1 in acto–S1. Some reversal of the localized perturbation in the actin-bound S1 apparently occurs when nucleotides bind to form the ternary complex acto–S1·ADP. This reversal is detected by AF but not by SAL. The structure of S1 in the ternary complex is not likely identical with that in S1·ADP in spite of the observed fluorescence levels of AF in both species being the same. If this were the case, the fluorescence of SAL in the ternary complex would have to be similar to that of S1-SAL·ADP. This was not observed. Similarly, the structure of the ternary complex is unlikely the same as in acto–S1 as the fluorescence of acto–S1-SAL·ADP would suggest. Clearly, the structure of the ternary complex is different from that of the two binary complexes, S1·ADP and acto–S1. The observed fluorescence data can be interpreted in terms of two states of ternary complexes. One state (T state) has a localized SH_1 structure that is considerably less open than in S1, giving rise to an enhanced internal quenching of AF fluorescence, and the other state (R state) has a structure that is somewhat more open in comparison with S1 and in which the AF fluorescence is less quenched by internal groups than in S1. Thus, the T state has a low AF fluorescence, and the R state has a high AF fluorescence. The observed low level of AF fluorescence in the ternary complex acto–S1-AF·ADP reflects an equilibrium between the two states. When SAL is the attached probe in the T state, its fluorescence should be higher than in S1-SAL because the probe is now more protected from solvent collision than in S1-SAL; in the R state, SAL should become more exposed, and its fluorescence would be quenched. If the enhancement of SAL in the T state is more than compensated by the quenching in the R state, the net fluorescence level would be low in comparison with that of S1-SAL. This would explain the apparent lack of fluorescence change with acto–S1-SAL upon addition of nucleotides. Several lines of kinetic evidence have suggested the existence of two types of ternary complexes (Geeves et al., 1984). They generally correspond to the weak and strong actin binding states of the myosin–nucleotide complexes (Eisenberg & Greene, 1980). These two states have been incorporated into the general scheme of the actomyosin ATPase cycle. Previous studies provided no indication on the structural difference between the two states of ternary complexes. The present results suggest a structural difference in terms of the local environment of the SH_1 region. These results do not rule out the possibility of a difference in the conformation of actin. If the difference indeed lies in the myosin conformation, as we suggest here, unbound myosin or myosin·ADP must be able to exist in similar conformations. Evidence for more than one S1·ADP conformation has been provided by NMR studies (Shriver & Sykes, 1982) carried out at different temperatures and by the lifetimes of ϵADP bound to S1 (Rosenfeld & Taylor, 1984). Our study (unpublished results) of the effect of temperature on the decay of bound ϵADP also supports the existence of two conformations of S1–nucleotide.

We (Cheung et al., 1983) have previously shown fluorescence heterogeneity in 1,5-IAEDANS attached to SH_1. The evidence was based on results from measurements of acrylamide quenching of steady-state intensity and lifetime. The attached IAEDANS showed a single lifetime in the absence of quencher but two lifetimes in the presence of acrylamide

concentrations above 50 mM. The heterogeneity of the attached probes in the present work evident from steady-state Stern–Volmer plots is directly confirmed by lifetime results obtained in the absence of quencher. The origin of this heterogeneity is unclear. Although we cannot rule it out, the fractional contributions of the two emission components in both S1-AF and S1-SAL would make heterogeneous labeling unlikely. We have previously suggested that the fluorescence heterogeneity observed with the IAEDANS probe may reflect labeling of heavy-chain-based isoenzyme (Cheung et al., 1983). The possibility of such labeling deserves further attention in future work since isolation of such heavy-chain-based S1 isoenzyme has recently been reported (Burke et al., 1986).

The dissociation constant of ADP for acto–S1-AF (1.6 μM) is considerably lower than the values previously published using unmodified S1, 200 μM (White, 1977) and 143 μM (Greene & Eisenberg, 1980). Apparently, fluorescein labeling greatly reduces the dissociation rate constant of ADP from acto–S1-AF (Ando, 1984), and the reduction could be due to interaction of the nucleotide with the fluorophore itself. While the rate of ADP dissociation from acto–S1-SAL is not known, it is reasonable to assume that it is also significantly reduced because the dissociation constants from both acto–S1-AF and acto–S1-SAL are very similar. Since it is known that bound nucleotide can be trapped by cross-linking SH_1 and SH_2 (Wells & Yount, 1982), it is not entirely surprising that modification of SH_1 stabilizes bound nucleotide. The question, however, is why this stabilization is observed only with acto–S1 and not with S1 unattached to actin. Since SH_1 is very close to the region of S1 heavy chain that binds actin with a high affinity (Katoh et al., 1985), interaction of actin with S1 at this high-affinity site may induce a perturbation that is transmitted to the vicinity of SH_1. This perturbation in turn could produce a constraint on the attached probe to stabilize the bound nucleotide. This model would require considerable interaction between the nucleotide site and SH_1 and would suggest that the tight binding of ADP to the labeled acto–S1 may be an in vitro property of the system.

S1-AF appears to be more sensitive to the interaction of the protein with polyvalent anions than S1-SAL. Since the effect of anions on S1-AF seems to saturate at the millimolar concentration range, it is rather unlikely that the anions act directly as quenchers of the fluorophore. A direct electrostatic interaction is also ruled out because the fluorescein moiety is not positively charged. The fact that the effects of ADP and these anions on S1-AF are not additive would suggest that both types of ligands induce a common effect in the environment of the fluorophore by competing for the same site within the nucleotide binding region. Consistent with this possibility are preliminary results showing that addition of AMP-PNP also induced a rapid decrease in fluorescence, such as always observed with ATP or ADP. This initial decrease, however, was followed by a slow increase. Such a biphasic change was not observed with S1-SAL. At this point, it is useful to recall a differential property of S1-AF in response to ADP and anions. Association of F-actin with S1-AF–ADP does not produce a change in fluorescence, whereas binding of actin to S1-AF–anion increases the fluorescence by as much as in the absence of anions (pyrophosphate is an exception). We do not know whether F-actin induces dissociation of bound anions or just cancels the effect of the anions still bound to the protein.

As a polyvalent anion, vanadate itself decreased the fluorescence intensity of S1-AF, but the slow fluorescence change which followed the formation of S1-AF·ADP·Vi probably represents a conformational change not only restricted to the vanadate attachment point but also extending to the entire nucleotide binding site. As depicted in Figure 4, the same ternary complex S1·ADP·Vi can be formed through either of two routes. This initial complex that is obtained with labeled S1 has a fluorescence state which is identical with that of S1·ADP obtained with labeled S1 and has a less open structure in the SH_1 region than S1. Transition of the initial complex to the final stable state S1*·ADP·Vi results in a more open structure than S1·ADP·Vi. This final structure is at least as open as that in S1-SAL as sensed by SAL, or more open than in S1-AF as monitored by AF. Recently, Rosenfeld and Taylor (1984) have demonstrated that the slow transition of S1·ϵADP·Vi to a stable complex is accompanied by a decrease in accessibility of the bound nucleotide to quencher acrylamide. These workers indicated that the ϵADP fluorescence was enhanced by Vi and the rate of this enhancement was 8.6×10^{-3} s^{-1}. An iodoacetamido-based spin-label attached to SH_1 was also used (Wells & Bagshaw, 1984) to characterize the complex formed between ADP, Vi, and myosin. These workers reported a slow transition which occurred after formation of the ternary complex M·ADP·Vi with a rate constant of 8.3×10^{-3} s^{-1}. Finally, we also observed a slow decrease of the S1 intrinsic fluorescence with S1·ADP·Vi. The small difference in this fluorescence between S1·ADP·Vi and S1*·ADP·Vi made it difficult to evaluate the rate constant. Different approaches have yielded evidence for the formation of a ternary complex between myosin, ADP, and Vi, and for the transition of the initial complex to a stable form with a rate constant in the range $(3–10) \times 10^{-3}$ s^{-1}. The sensitivity provided by the extrinsic fluorescence can be useful to characterize conformational changes in the complex S1–ADP·Vi believed to mimic a transient intermediate in the ATP hydrolysis.

References

Ando, T. (1984) *Biochemistry 23*, 375–381.

Botts, J., Ue, K., Hozumi, T., & Samet, J. (1979) *Biochemistry 18*, 5157–5163.

Burke, M., Purvis, S. F., & Sivaramakrishnan, M. (1986) *J. Biol. Chem. 261*, 253–256.

Cheung, H. C., Gonsoulin, F., & Garland, F. (1983) *J. Biol. Chem. 258*, 5775–5786.

Cheung, H. C., Gonsoulin, F., & Garland, F. (1985) *Biochim. Biophys. Acta 832*, 52–62.

Duke J., Takashi, R., Ue, K., & Morales, M. F. (1976) *Proc. Natl. Acad. Sci. U.S.A. 73*, 302–306.

Durbin, J., & Watson, G. S. (1951) *Biometrika 38*, 1159–178.

Eisenberg, E., & Greene, L. (1980) *Annu. Rev. Physiol. 42*, 293–309.

Flamig, D. P., & Cusanovich, M. A. (1981) *Biochemistry 20*, 6760–6767.

Geeves, M. A., Goody, R. S., & Gutfreund, H. (1984) *J. Muscle Res. Cell Motil. 5*, 351–361.

Goodno, C. C. (1979) *Proc. Natl. Acad. Sci. U.S.A. 76*, 2620–2624.

Goodno, C. C. (1982) *Methods Enzymol. 85*, 116–123.

Greene, L. E., & Eisenborg, (1980) *J. Biol. Chem. 255*, 534–548.

Houk, T. W., & Ue, K. (1974) *Anal. Biochem. 62*, 66–74.

Katoh, T., Katoh, H., & Morita, F. (1985) *J. Biol. Chem. 260*, 6723–6727.

Konrad, M., & Goody, R. S. (1982) *Eur. J. Biochem. 128*, 547–555.

Lowry, O, H., Rosebrough, N. J., Farr, A. L., & Randall, R. J. (1951) *J. Biol. Chem. 193*, 265–275.

Marsh, D. J., & Lowey, S. (1980) *Biochemistry 19*, 774–784.

Morales, M. F., Borejdo, J., Botts, J., Cooke, R., Mendelson, R. A., & Takashi, R. (1982) *Annu. Rev. Phys. Chem. 33*, 319–351.
Mornet, D., Bertrand, R., Pantel, P., Audemard, E., & Kassab, R. (1979) *Biochem. Biophys. Res. Commun. 89*, 925–932.
Mulrad, A., & Morales, M. E. (1984) *Proc. Natl. Acad. Sci. U.S.A. 81*, 1003–1007.
Reisler, E. (1982) *Methods Enzymol. 85*, 84–93.
Rosenfeld, S. S., & Taylor, E. W. (1984) *J. Biol. Chem. 259*, 11920–11929.
Sekine, T., & Kielley, W. (1964) *Biochim. Biophys. Acta 81*, 336–345.
Shriver, J. W., & Sykes, B. D. (1982) *Biochemistry 21*, 3022–3028.
Spudich, J. A., & Watts, S. (1971) *J. Biol. Chem. 246*, 4866–4871.
Stern, O., & Volmer, M. (1919) *Phys. Z. 20*, 183–188.
Wagner, P. D., & Weeds, A. G. (1977) *J. Mol. Biol. 109*, 455–473.
Weeds, A. G., & Taylor, R. S. (1975) *Nature (London) 257*, 54–56.
Wells, C., & Bagshaw, C. R. (1984) *J. Muscle Res. Cell Motil. 5*, 97–112.
Wells, J. A., & Yount, R. G. (1982) *Methods Enzymol. 85*, 93–116.
White, H. D. (1977) *Biophys. J. 17*, 40a.
Wiedner, H., Wetzel, R., & Eckstein, F. (1978) *J. Biol. Chem. 253*, 2763–2768.

Preparation of a High-Affinity Photolabeling Reagent for the Gal/GalNAc Lectin of Mammalian Liver: Demonstration of Galactose-Combining Sites on Each Subunit of Rabbit Hepatic Lectin†

Reiko T. Lee* and Yuan Chuan Lee
Department of Biology, The Johns Hopkins University, Baltimore, Maryland 21218
Received June 17, 1986

ABSTRACT: On the basis of the knowledge that the D-galactose/*N*-acetyl-D-galactosamine-specific lectin of rabbit liver can tolerate a large group on the C-6 hydroxyl group of a galactoside [Lee, R. T. (1982) *Biochemistry 21*, 1045–1050], we prepared a high-affinity photolabeling reagent for this lectin from a triantennary glycopeptide fraction of asialofetuin. The C-6 hydroxyl group of a D-galactopyranoside was converted, under mild conditions, into a primary amino group. The procedure involves conversion of the hydroxyl group to an oxo group with galactose oxidase, followed by reductive amination using benzylamine and sodium cyanoborohydride. Catalytic hydrogenolysis of the benzylamino derivative yielded the desired 6-amino-6-deoxy-D-galactoside. A 4-azidobenzoyl group was attached to the newly produced amino group to yield a photoactivatable affinity-labeling reagent. The reagent labeled the Triton-solubilized, purified hepatic lectins of rabbit and rat in a *photo-* and *affinity*-dependent manner. All the polypeptide subunits of the lectins were labeled, indicating that each subunit contains at least one D-galactose-combining site. In the case of the rabbit hepatic lectin, the minor subunit (46 kDa) was labeled more efficiently than the major one (40 kDa).

The Gal/GalNAc-specific[1] lectin of mammalian livers (also known as the "asialoglycoprotein receptor") is a transmembrane protein present on the cell surface and the internal membranes of hepatocytes (Pricer & Ashwell, 1976; Harford & Ashwell, 1981; Chiacchia & Drickamer, 1984). The lectin has been purified in a detergent-solubilized form by affinity chromatography from livers of several mammalian species (Hudgin et al., 1974; Pricer & Ashwell, 1976; Baenziger & Maynard, 1980; Bezouska et al., 1985). The Triton-solubilized lectins from different species all exist as large molecular species (>200 kDa), composed of subunits of 40–60 kDa in size that are not held together by disulfide bonds. Although the lectin is capable of binding monovalent galactosides[2] ($K_d = 10^{-3}$–10^{-4} M), proper clustering of galactosyl residues within the ligand structure increases the affinity to the lectin enormously (Baenziger & Fiete, 1980; Connolly et al., 1982; Lee et al., 1983; Lee, R. T., et al., 1984). For instance, the Gal-terminated triantennary and tetraantennary oligosaccharides that exist in desialylated serum glycoproteins, such as asialoorosomucoid and asialofetuin, manifest up to a millionfold higher affinity toward this lectin on the hepatocyte surface than a simple galactoside, although the actual Gal concentration is increased by only 3–4-fold (Lee et al., 1983). The dramatic increase in affinity by clustering of sugars seems to be a unique property of the hepatic Gal/GalNAc lectin and possibly other animal lectins (Hoppe & Lee, 1983; Kuhlenschmidt & Lee, 1984).

†Supported by USPHS NIH Research Grants AM9970 and CA21901. Publication No. 1333 from the McCollum-Pratt Institute, The Johns Hopkins University.

[1] Abbreviations: ASOR, asialoorosomucoid; BOC, *tert*-butyloxycarbonyl; BSA, bovine serum albumin; Me_2SO, dimethyl sulfoxide; HEPES, *N*-(2-hydroxyethyl)piperazine-*N*′-2-ethanesulfonic acid; PAGE, polyacrylamide gel electrophoresis; SDS, sodium dodecyl sulfate; TLC, thin-layer chromatography; EDTA, ethylenediaminetetraacetic acid; Gal, galactose; GalNAc, *N*-acetylgalactosamine; Tris-HCl, tris(hydroxymethyl)aminomethane hydrochloride.

[2] Unless otherwise specified, all sugars are of the D configuration and in pyranose form, and all amino acids are of the L configuration.

0006-2960/86/0425-6835$01.50/0